Friction **1**(1): 41–62 (2013)
DOI 10.1007/s40544-013-0005-3 ISSN 2223-7690

REVIEW ARTICLE

Method of reduction of dimensionality in contact and friction mechanics: A linkage between micro and macro scales

Valentin L. POPOV*

Berlin University of Technology, Berlin 10623, Germany

Received: 27 October 2012 / Revised: 31 January 2013 / Accepted: 18 February 2013

Abstract: Computer simulations have been an integral part of the technical development process for a long time now. Industrial tribology is one of the last fields in which computer simulations have, until now, played no significant role. This is primarily due to the fact that investigating tribological phenomena requires considering all spatial scales from the macroscopic shape of the contact system down to the micro-scales. In the present paper, we give an overview of the previous work on the so-called method of reduction of dimensionality (MRD), which in our opinion, gives a key for the linking of the micro- and macro-scales in tribological simulations.

MRD in contact mechanics is based on the mapping of some classes of three-dimensional contact problems onto one-dimensional contacts with elastic foundations. The equivalence of three-dimensional systems to those of one-dimension is valid for relations of the indentation depth and the contact force and in some cases for the contact area. For arbitrary bodies of revolution, MRD is exact and provides a sort of "pocket edition" of contact mechanics, giving the possibility of deriving any result of classical contact mechanics with or without adhesion in a very simple way.

A tangential contact problem with and without creep can also be mapped exactly to a one-dimensional system. It can be shown that the reduction method is applicable to contacts of linear visco-elastic bodies as well as to thermal effects in contacts. The method was further validated for randomly rough self-affine surfaces through comparison with direct 3D simulations.

MRD means a huge reduction of computational time for the simulation of contact and friction between rough surfaces accounting for complicated rheology and adhesion. In MRD, not only is the dimension of the space reduced from three to one, but the resulting degrees of freedom are independent (like normal modes in the theory of oscillations). Because of this independence, the method is predestinated for parallel calculation on graphic cards, which brings further acceleration. The method opens completely new possibilities in combining microscopic contact mechanics with the simulation of macroscopic system dynamics without determining the "law of friction" as an intermediate step.

Keywords: contact mechanics; rough surfaces; static friction; sliding friction; elastomers; adhesion; rolling; dynamic tangential contacts; reduction of dimensionality; scale linkage

1 Introduction

We live in an age of information technology. Numerical simulation methods have become a solid foundation for technological development processes. In many fields, such as structures and fluid dynamics, numerical methods can no longer be overlooked. Tribology is one of the last bastions of engineering sciences where numerical methods have been as good as non-existent in development and optimization. When dealing with friction or wear, the simple Coulomb's law of friction is always drawn upon, even until today: friction force is proportional to

* Corresponding author: Valentin L. POPOV.
E-mail: v.popov@tu-berlin.de

normal force with an empirical coefficient of friction that is dependent only on the material pairing. It is no secret that this law is only a very rough approximation. The coefficient of friction can change by a factor of 4 or more for the same material pairing, dependent on normal force, contact configuration, speed, and roughness. However, there exist no reliable simulation strategies that allow for the friction force to be calculated for specific systems. The main reason for this lies in the multi-scaled characteristics of the friction phenomenon. For example, a monolayer of impurity atoms on a metal surface changes both friction and wear dramatically. On the other hand, the contact mechanics of real surfaces is controlled by spatial scales differing by many orders of magnitude. In particular, the plastic behavior will be different on different spatial scales. The same problems arise in simulation of rubber: the rolling resistance and the wear in this material can be caused by spatial and time scales differing by about 10 orders of magnitude because of spatial and frequency dependence of the rheological properties of rubber. A correct simulation of such systems must take all of these scales into account. The multi-scale nature of tribological systems begins with the fractal character of their roughness. Since Bowden and Tabor [1], one knows that surface roughness plays a decisive role in tribological contacts. Already in the 50's of the 20th century it became clear that many surfaces of interest (e.g., fracture surfaces, wear surfaces, or surfaces produced with typical manufacturing methods) are fractal surfaces showing roughness on all scales from atomic to macroscopic [2, 3]. This leads to the sensitivity of the contact properties on small scales to those on larger scales and finally to the dependence of friction both on macroscopic loading conditions and processes occurring on the smallest microscopic scale [4, 5].

The current processing speeds of modern computers are far from sufficient to simulate contact and friction phenomena for real surfaces while considering all relevant scales. Therefore, it is important to search for simulation methods which accept the loss of information about parts of the system but allow for a small number of especially meaningful macroscopic quantities to be quickly calculated. This technique is, of course, in no way new and is actually the tried and true method that science has followed since its inception. In the field of contact mechanics for real surfaces, one such possibility provides the method of reduction of dimensionality (MRD). The method of reduction of dimensionality was proposed in 2005 by Popov et al. [6] in a presentation at a workshop. Proceedings of this workshop appeared in 2007 as a special issue of Tribology International [7].

MRD is based on the observation that close analogies exist between certain types of three-dimensional contact problems and the simplest contacts with a one-dimensional elastic foundation. Thereby, it is important to emphasize that this is not an approximation: The properties of one-dimensional systems coincide exactly with those of the original three-dimensional system. The price for this reduction is high, but for many applications quite acceptable. One obtains the exact results only for the relationships between the force, the (macroscopic) relative displacement of the bodies, and the contact radius. With this, all quantities that depend on the force-displacement relationship can be calculated. In the area of exact agreement, parameters such as the contact stiffness and the corresponding electrical resistance [8] and thermal conductivity can be found. In the case of elastomers, dissipated energy and friction forces also belong to this set. The applicability of the MRD was extended in 2007 to contacts between randomly rough surfaces [9, 10], viscoelastic bodies [11], and frictional problems [12−16]. The method has been successfully applied to dynamic tangential [17, 18] and rolling [19, 20] contacts. An important step was made in 2011 by M. Heß, in which he provided a rigorous proof for the applicability of the method of reduction of dimensionality for arbitrary rotationally symmetric bodies [21, 22] both with and without adhesion.

2 Basic ideas

We limit our consideration to "typical tribological systems" which are characterized by the laws of dry friction being approximately met. This implies that the real contact area remains much smaller than the apparent contact area or the apparent contact area is much smaller than the size of the tribological system as a whole. For "typical tribological systems,"

there is a series of properties that allow for immense simplification of the contact problem and in this way, allow quick calculation even in multi-scaled systems. The simplifying properties used in the reduction method are the following [5]:

(a) For velocities much smaller than the speed of sound, deformations in the relevant vicinity of the contact area determining the contact forces can be treated as quasi-static.

(b) The potential energy, and therefore, the force-displacement relation, is a local property that depends only on the configuration of the surfaces at the distances of the order of magnitude of the size of the contact area and not on the form or size of the body as a whole. The locality does not mean that the elastic coupling of different points in the contact area is not considered.

(c) The kinetic energy, on the other hand, is a "global property" that depends only on the form and size of the body as a whole and not on the configuration of the micro-contacts.

The last two properties mean that the "elastic properties" and the "inertia properties" are completely decoupled, the first being purely microscopic and the latter, purely macroscopic. The above three properties are found in many macroscopic tribological systems. The application area of the subsequent methods is, accordingly, very wide.

Another crucial property of contacts between three-dimensional bodies is the close similarity between these contacts and certain one-dimensional problems. The fundamental ideas of this analogy are presented in the following. If a cylindrical indenter is pressed into the surface of an elastic continuum (Fig. 1a), then the stiffness k of the contact is proportional to its diameter D [5]:

$$k = DE^* \tag{1}$$

Where E^* is the effective elastic modulus

$$\frac{1}{E^*} = \frac{1-\nu_1^2}{E_1} + \frac{1-\nu_2^2}{E_2} \tag{2}$$

E_1 and E_2 are the Young's moduli of contacting bodies, and ν_1 and ν_2, their Poisson-ratios. The proportionality of the stiffness to the diameter can be reproduced using a one-dimensional elastic foundation (Fig. 1b). In order to fulfill Eq. (1), the stiffness per unit length must be chosen as E^*. Every individual spring must have the stiffness

$$\Delta k_z = E^* \Delta x \tag{3}$$

where Δx is the distance between the springs of the elastic foundation and z is the vertical coordinate.

The tangential stiffness of a three-dimensional contact is also proportional to the diameter of the contact [5]:

$$k_x = DG^* \tag{4}$$

where

$$\frac{1}{G^*} = \frac{(2-\nu_1)}{4G_1} + \frac{(2-\nu_2)}{4G_2} \tag{5}$$

G_1 and G_2 are the shear moduli of the contacting bodies. For the same reasons as in the case of a normal contact, the tangential contact can be replicated using a one-dimensional elastic foundation. The tangential stiffness of individual springs in the elastic foundation must be chosen according to

$$\Delta k_x = G^* \Delta x \tag{6}$$

Note that throughout this paper, we assume that the contacting materials satisfy the condition of "elastic similarity"

$$\frac{1-2\nu_1}{G_1} = \frac{1-2\nu_2}{G_2} \tag{7}$$

guaranteeing the decoupling of the normal and tangential contact problems [23]. In particular, this condition is always satisfied in the important case of the contact between a rigid body and an incompressible elastomer (both sides of Eq. (7) are then zero).

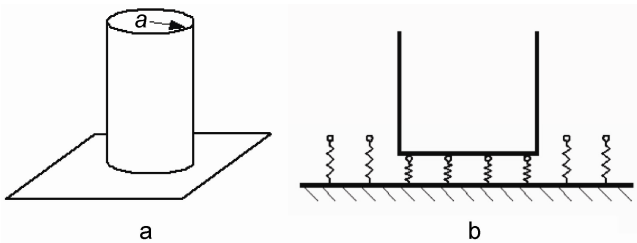

Fig. 1 (a) Contact of a rigid cylindrical indenter with an elastic half-space and (b) its one-dimensional representation.

3 The rule of Geike & Popov and the rule of Heß for normal contacts

Amazingly, the contact with an elastic foundation defined with Eq. (3) gives correct force-displacement relations not only for cylindrical indenters but also for a large class of simple surface profiles. However, the surface profile must be modified according to some simple rules. For parabolic (or spherical) profiles, the rule was given by Geike and Popov [9]. They have shown that the relations between force, indentation depth, and contact radius of a spherical indenter with radius R pressed into a half-space (Fig. 2a) can be reproduced exactly with a contact with a one-dimensional elastic foundation (Fig. 2b) by changing the radius. If a "sphere" with the radius R_1 is brought into contact with the elastic foundation (penetration depth d), then the following contact quantities result: The contact radius is equal to

$$a = \sqrt{2R_1 d} \tag{8}$$

and the normal force is

$$F_N(d) = \frac{4\sqrt{2}E^*}{3}\sqrt{R_1 d^3} \tag{9}$$

If we choose a radius

$$R_1 = R/2 \tag{10}$$

then the Eqs. (8) and (9) coincide exactly with Hertzian theory. The Eq. (10) means that the cross-section of the three-dimensional profile is stretched by the factor of 2 in the vertical direction (*Rule of Geike & Popov*).

In 2011, Heß showed that the exact mapping of contact problems to one-dimensional elastic foundations is possible for arbitrary bodies of revolution [21, 22]. If a body of revolution is described by the equation $z = z(r)$, then a one-dimensional profile

$$z_{1D}(x) = x\int_0^x \frac{z'(r)}{\sqrt{x^2 - r^2}}\mathrm{d}r \tag{11}$$

in contact with an elastic foundation defined by Eq. (3) will have exactly the same contact properties as the original three-dimensional contact. In the case when the three-dimensional profile is described by a power-function

$$z(r) = c_n r^n \tag{12}$$

the equivalent one-dimensional profile is a power-function with the same power, but a modified coefficient:

$$z_{1D}(x) = \mathrm{c_n}\, x\int_0^x \frac{nr^{n-1}}{\sqrt{x^2 - r^2}}\mathrm{d}r = \tilde{\mathrm{c}}_\mathrm{n}\, x^n \tag{13}$$

where

$$\tilde{c}_n = \kappa_n c_n \tag{14}$$

and

$$\kappa_n = n\int_0^1 \frac{\xi^{n-1}}{\sqrt{1-\xi^2}}\mathrm{d}\xi = \frac{\sqrt{\pi}}{2}\frac{n\Gamma(\frac{n}{2})}{\Gamma(\frac{n}{2}+\frac{1}{2})} \tag{15}$$

$\Gamma(n)$ is the Gamma-function

$$\Gamma(n) = \int_0^\infty t^{n-1}e^{-t}dt \tag{16}$$

In particular, for a cone ($n = 1$) we get $\kappa_1 = \pi/2$ and for a parabolic profile ($n = 2$) $\kappa_2 = 2$. Note that the power n is an arbitrary positive number (it does not

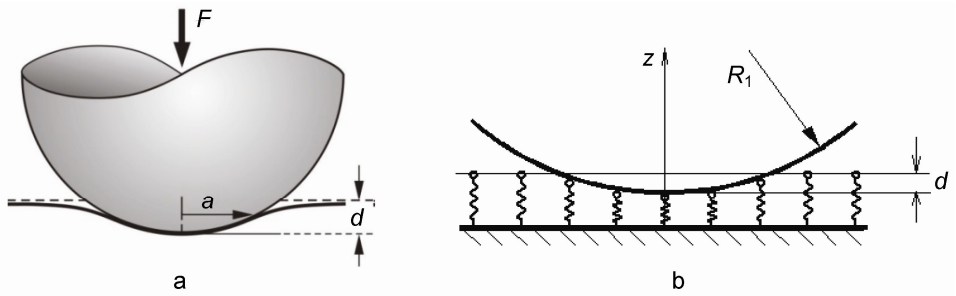

Fig. 2 Contact of a spherical indenter with a half-space and its one-dimensional representation.

need to be an integer).

The general reason for the possibility of mapping three-dimensional contacts with bodies of revolution onto one dimension is simple, and it is instructive to discuss it. Let us first consider a rigid indenter having the form described by a power law

$$z(r) = c_n r^n \tag{17}$$

which is pressed to a depth d into an elastic half-space. The unit of the coefficient c_n is $[m]^{1-n}$. As the equilibrium equations of elasticity do not contain any quantities with the dimension of length, it follows from dimensional analysis that the contact radius a can only be a function of the indentation depth of the form

$$a \propto c_n^{\alpha} d^{1-\alpha(1-n)} \tag{18}$$

with an arbitrary constant exponent α. On the other hand, if the Eq. (17) is stretched in the horizontal plane by a factor of C ($r = r'C$) and at the same time in the vertical direction by the factor of C^n ($z = z'C^n$), then the profile does not change at all. The contact radius in the new coordinates scales as C^{-1} and the indentation depth remains unchanged. From Eq. (18), it follows that $C^{-1} = C^{\alpha n}$ and $\alpha = -1/n$. Thus, the contact radius should be a power function of the indentation depth of the form

$$a \propto \left(d / c_n\right)^{1/n} \tag{19}$$

Once the dependence of the contact radius on the indentation depth is known, the dependence of the normal force follows straightforwardly. Indeed, the differential contact stiffness depends only on the current configuration of the contact and is given by the same equation as for a cylindrical indenter (see Ref. [5] or Ref. [24] for the proof):

$$\frac{\partial F_N}{\partial d} = 2aE^* \tag{20}$$

With Fomula (19), it follows that

$$F_N \propto \frac{2E^*}{(1+1/n)} c_n^{-1/n} d^{1+1/n} \tag{21}$$

In the one-dimensional case, it is trivial to see that both Fomula (19) and Eq. (20) remain valid. Thus, the power law (21) is valid as well, and it is only the question of the correct vertical scaling to obtain exactly equivalent results. The scaling coefficient can only depend on the power n. The existence of a linear mapping for an arbitrary power-function means that, for a general profile, the function must have the form of a linear integral transformation. The form of this transformation is given by Eq. (11).

To illustrate the simplicity and the efficiency of the method of reduction of dimensionality, let us consider a contact of a flattened parabolic indenter

$$z(r) = \begin{cases} 0, & \mathrm{r} < a_0 \\ \dfrac{r^2 - a_0^2}{2R}, & \mathrm{a}_0 < r \end{cases} \tag{22}$$

with an elastic half-space; a_0 is here the radius of the flattening. The corresponding one-dimensional profile is given by Eq. (11):

$$z_{1D}(x) = \begin{cases} 0, & |x| < a_0 \\ \dfrac{|x|\sqrt{x^2 - a_0^2}}{R}, & a_0 < |x| \end{cases} \tag{23}$$

The interrelation of the indentation depth d and the contact radius a is given by the condition

$$d = z_{1D}(a) = \frac{a\sqrt{a^2 - a_0^2}}{R} \tag{24}$$

The normal force is then equal to

$$F_N(a) = 2E^* \int_0^a (z_{1D}(a) - z_{1D}(x))\,\mathrm{d}x = \frac{2E^*}{3R}\sqrt{a^2 - a_0^2}\,(2a^2 + a_0^2) \tag{25}$$

The Eqs. (24) and (25) are exact solutions for the three-dimensional contact first found by Ejike in 1981 [25].

4 Stress distribution in the contact area

Heß further found that the pressure distribution in a real three-dimensional contact can be reconstructed from the linear force density $q(x) = \Delta f(x)/\Delta x$, found in the one-dimensional model, where $\Delta f(x)$ is the normal force in a spring having the coordinate x. According to Heß, the pressure distribution is given

by the Abel transformation [21, 22]:

$$p(r) = -\sigma_{zz}(r) = -\frac{1}{\pi}\int_r^\infty \frac{q'(x)}{\sqrt{x^2 - r^2}}\mathrm{d}x \tag{26}$$

For example, in the case of a cylindrical indenter, the force density $q(x)$ is constant inside the contact interval:

$$q(x) = \begin{cases} F_N/(2a), & |x| < a \\ 0, & |x| > a \end{cases} \tag{27}$$

Therefore, $q'(x) = -\frac{F_N}{2a}(\delta(x+a) - \delta(x-a))$ and Eq. (26) gives

$$\begin{aligned} p &= \frac{1}{\pi}\frac{F_N}{2a}\int_r^\infty \frac{(\delta(x+a) - \delta(x-a))}{\sqrt{x^2 - r^2}}\mathrm{d}x \\ &= \begin{cases} \frac{F_N}{2\pi a^2}\frac{1}{\sqrt{1-(r/a)^2}}, & |r| < a \\ 0, & |r| > a \end{cases} \end{aligned} \tag{28}$$

which is exactly the stress distribution in a three-dimensional contact with a cylindrical indenter of radius a (see, for example, Ref. [23]). Similarly, for the parabolic case, the force density in the one-dimensional case is calculated trivially to be

$$q(x) = E^*\left(d - x^2/(2R_1)\right), \quad \text{for} \quad |x| < a = \sqrt{2R_1 d} \tag{29}$$

For the derivative, we get $q'(x) = E^* x/R_1$. Substitution into Eq. (26) gives

$$\begin{aligned} p &= \frac{E^*}{\pi R_1}\int_r^\infty \frac{x\mathrm{d}x}{\sqrt{x^2 - r^2}} = \frac{E^*}{\pi R_1}\int_r^a \frac{x\mathrm{d}x}{\sqrt{x^2 - r^2}} \\ &= \frac{2}{\pi}E^*\left(\frac{d}{R}\right)^{1/2}\sqrt{1-(r/a)^2} \end{aligned} \tag{30}$$

which is exactly the result for the Hertzian problem. As the last example, let us consider the contact between a conical indenter with the slope θ and an elastic half- space. The force density is calculated as

$$q(x) = E^*\left(d - \frac{\pi}{2}|x|\tan\theta\right), \quad \text{for} \quad |x| < a = \frac{2d}{\pi\tan\theta} \tag{31}$$

For the derivative, we get $q(x)' = -E^*\frac{\pi}{2}\mathrm{sgn}(x)\cdot\tan\theta$. Substitution into Eq. (26) gives

$$p = \frac{E^*\tan\theta}{2}\int_r^a \frac{dx}{\sqrt{x^2 - r^2}} = \frac{E^*\tan\theta}{2}\ln\left(\frac{a}{r} + \sqrt{\left(\frac{a}{r}\right)^2 - 1}\right) \tag{32}$$

This result coincides with the exact stress distribution in a contact with a conical indenter [24].

Equation (26) gives the exact stress distribution, not only in these simple classic cases but for *arbitrary* bodies of revolution, provided the rule of Heß (Eq. (11)) has been applied for modification of the profile.

5 Normal contacts with adhesion

Heß succeeded in 2011 in generalizing the reduction method to adhesive contacts of elastic solids. He considered the boundary of adhesive contact as a Griffith's crack [26] in an ideally elastic body. His argument was very simple and elegant: It is known that the stress distribution in an adhesive contact described by the classical JKR theory [27] is a superposition of a pressure distribution with a parabolic indenter and a negative stress distribution by the "rigid pulling" of the contact area. As both of these contact problems can be mapped exactly onto one dimension, this should be valid for the entire adhesive problem as well. The rule of Heß for adhesive contacts is the following: If we first press a modified indenter (Eq. (11)) into the elastic foundation and then pull it off as shown in Fig. 3, then the springs will detach when the following critical elongation is achieved [21, 22, 28]:

$$\Delta l_{\max}(a) = \sqrt{\frac{2a\pi\gamma_{12}}{E^*}} \tag{33}$$

Note that this criterion is non-local, as it depends on the actual radius of the contact region.

As a simple example let us consider an adhesive contact between a rigid cylinder with a radius a and elastic half-space (Fig. 4). In this case, all springs will detach at the instant in which all of them achieve the critical elongation (33). The total normal force which must be applied to achieve this state is just

$$F_A = 2aE^*\sqrt{\frac{2a\pi\gamma_{12}}{E^*}} = \sqrt{8E^* a^3\pi\gamma_{12}} \tag{34}$$

which is also the exact three-dimensional result for this adhesive problem [21].

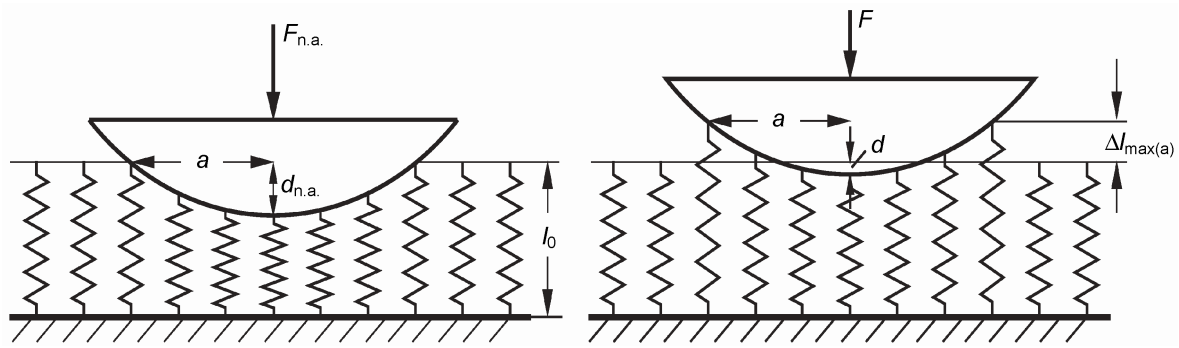

Fig. 3 Adhesive contact during the pressing and detaching phases.

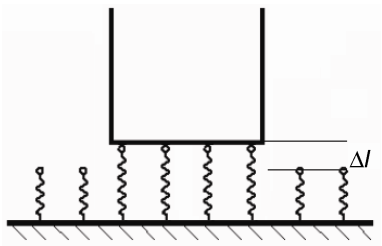

Fig. 4 The one-dimensional equivalent system for the adhesive contact between a rigid cylinder and an elastic half-space.

As a second example, let us calculate the adhesion force with a conical indenter with the slope θ. The vertical displacement of the springs with coordinate x is now $u(x) = d - \frac{\pi}{2}|x|\tan\theta$. The contact radius is given by the condition $u(a) = -\Delta l_{\max}(a)$, resulting in

$$d = \frac{\pi}{2} a \tan\theta - \sqrt{\frac{2a\pi\gamma_{12}}{E^*}} \tag{35}$$

The normal force is given by

$$F_N = 2E^* \int_0^a \left(d - \frac{\pi}{2} x \tan\theta \right) \mathrm{d}x = E^* \left(\frac{\pi a^2}{2} \tan\theta - 2a\sqrt{\frac{2a\pi\gamma_{12}}{E^*}} \right) \tag{36}$$

Its minimum value is $-F_A$ with

$$F_A = \frac{54\gamma_{12}^2}{\pi E^* \tan^3\theta} \tag{37}$$

which coincides with the solution of the 3D adhesive contact problem [21].

Similar calculations for a parabolic profile would lead to the classical JKR result $F_A = (3/2)\pi R\gamma_{12}$.

Application of the rule of Heß (Eq. (33)) provides not only exact adhesive forces for an arbitrary body of revolution but also the complete force-displacement dependence and force-contact radius dependence. The proof can be found in Refs. [21, 22]. The above formulation of the adhesive contact is, however, only applicable to a contact of elastic bodies. For viscoelastic bodies, the idea of treating an adhesive contact as a crack can be used too, but the *process zone* in the vicinity of the crack opening should be considered in detail, as first done by Prandtl [29]. A more detailed discussion of adhesion in elastomers can be found in Ref. [30]. Application of the method of reduction of dimensionality to viscoelastic adhesive contacts is described in Ref. [31].

Adhesive properties (adhesion force and adhesion coefficient) of contacts between elastic bodies with rough surfaces have been investigated in Ref. [32]. The authors constructed adhesion maps showing the dependence of adhesive properties on the roughness, rms slope of the surface, elastic modulus, surface energy, and fractal dimension.

6 Tangential contact

In this section, we would like to illustrate the application of the method of reduction of dimensionality using an example of a tangential contact with friction. A parabolic body is initially pressed into an elastic half-space with the normal force F_N and subsequently tangentially loaded with a force F_x (Fig. 5). It is assumed that the friction between the bodies can be described using the simple Coulomb's law of friction with a constant coefficient of friction. Due to the fact that at the edges of the contact area, the normal force

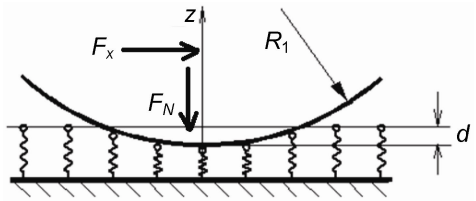

Fig. 5 Tangential contact with friction with a parabolic body.

in the springs disappears, a sliding domain exists here, while in the center of the contact area, as long as the tangential force is not too large, the surfaces stick. We denote the radius of the sticking domain with c.

The vertical displacement of a spring at a distance x from the center of the contact is

$$u_z(x) = d - \frac{x^2}{2R_1} \tag{38}$$

and the resulting spring force is

$$f_N(x) = E^* u_z(x)\Delta x = \left(d - \frac{x^2}{2R_1}\right) E^* \Delta x \tag{39}$$

The contact radius is determined from the condition $u_z(a) = 0$, and according to this, is equal to

$$a = \sqrt{2R_1 d} \tag{40}$$

We denote the horizontal displacement of the parabolic indenter relative to the substrate as u_x. Then, the force acting on a spring which sticks to the substrate is equal to

$$f_x(x) = \Delta k_x u_x = G^* \Delta x \cdot u_x \tag{41}$$

The boundaries of the sticking region are determined from the condition that the tangential force reaches the maximum possible value for the static friction force:

$$f_x(c) = \mu f_N(c) \tag{42}$$

or

$$G^* \Delta x \cdot u_x = \mu\left(d - \frac{c^2}{2R_1}\right) E^* \Delta x \tag{43}$$

From this, it follows that

$$c^2 = 2R_1\left(d - \frac{G^*}{E^*}\frac{u_x}{\mu}\right) \tag{44}$$

Solving for u_x results in

$$u_x = \mu \frac{E^*}{G^*}\left(d - \frac{c^2}{2R_1}\right) \tag{45}$$

The sliding in the remaining regions means that Coulomb's law of friction is fulfilled in these regions:

$$f_x(c) = \mu f_N(c), \quad \text{if } c < |x| < a \tag{46}$$

We now calculate the normal and tangential forces in this state. The normal force results in the Hertzian result:

$$F_N = \int_{-a}^{a}\left(d - \frac{x^2}{2R_1}\right) E^* \mathrm{d}x = \frac{4}{3} E^* (2R_1)^{1/2} d^{3/2} = \frac{2E^* a^3}{3R_1} \tag{47}$$

The tangential force is calculated as

$$\begin{aligned} F_x &= 2\int_0^c G^* u_x \mathrm{d}x + 2\int_c^a \mu\left(d - \frac{x^2}{2R_1}\right) E^* \mathrm{d}x \\ &= \frac{2E^* a^3 \mu}{3R_1}\left(1 - \left(\frac{c}{a}\right)^3\right) = \mu F_N \left(1 - \left(\frac{c}{a}\right)^3\right) \end{aligned} \tag{48}$$

From this, the relationship for the radius of the stick area results [5]:

$$\frac{c}{a} = \left(1 - \frac{F_x}{\mu F_N}\right)^{1/3} \tag{49}$$

which coincides with the three-dimensional result [5].

The maximum displacement until the point of complete sliding is given by Eq. (45) through the insertion of $c = 0$:

$$u_{x,\max} = u_x = \mu \frac{E^*}{G^*} d \tag{50}$$

and is likewise identical to the three-dimensional result.

It can be easily shown that the Abel-transformation (Eq. (26)) provides the correct stress distribution in a true three-dimensional tangential contact also in this case. The (tangential) force density is given in this case by the following relations:

$$q_x(x) = \begin{cases} \mu\left(d - \dfrac{x^2}{2R_1}\right) E^*, & c < |x| < a \\ G^* u_x, & |x| < c \\ 0, & |x| > a \end{cases} \tag{51}$$

In the sticking part of the contact, the force density is constant and can be represented as the difference between two force functions $q_x(x) = q_1(x) - q_2(x)$, where

$$\begin{aligned} q_1(x) &= \mu E^* \left[d - \frac{x^2}{2R_1} \right] = \frac{\mu E^*}{2R_1}\left(a^2 - x^2\right) \\ q_1(x) &= \mu E^* \left[\left(d - \frac{G^* u_x}{E^* \mu} \right) - \frac{x^2}{2R_1} \right] = \frac{\mu E^*}{2R_1}\left(c^2 - x^2\right) \end{aligned} \tag{52}$$

From this, it follows immediately that the three-dimensional stress distribution will be a difference between two "Hertzian-like" stress distributions, which is really the case in a true three-dimensional system [33, 34].

In 1995, Jäger [35] succeeded in showing that an arbitrary axial-symmetric tangential contact problem with friction can be mapped identically to the corresponding normal contact problem in the framework of the Cattaneo-Mindlin theory [33, 34]. This means that the exact mapping of 3D problems to those of one dimension is valid for tangential contacts of *arbitrary* bodies of revolution.

7 Frictional damping in an oscillating tangential contact

If the tangential load is oscillating, this leads to the slip in the area in the vicinity of the border of the contact area and to frictional damping. In this section we consider the frictional damping of an oscillating contact of a parabolic elastic body in contact with a rigid plane. We apply the method of reduction of dimensionality and show that the resulting energy dissipation is exactly the same as in the true 3D problem (solved in Ref. [36]).

Consider a spring with a normal stiffness k_z and tangential stiffness k_x, which is pressed against a rigid plane so that the approach is equal to δ. Assume a coefficient of friction μ between the spring and the plane. Now let the "free end" of the spring oscillate tangentially with an amplitude A (from $+A$ to $-A$). If the condition

$$F_x = Ak_x < \mu F_N = \mu\delta \cdot k_z \tag{53}$$

is fulfilled, then there is no relative movement between the spring and the plane and there is no energy dissipation. If however, the amplitude is larger then A_c:

$$A_c = \mu\delta \cdot \frac{k_z}{k_x} = \mu\delta \cdot \frac{2-\nu}{2(1-\nu)} \tag{54}$$

then the spring will stick until the displacement A_c is achieved and slip during the further part $A - A_c$. In the following, we carry out the calculation for the case $\nu = 1/3$:

$$A_c = \mu\delta \cdot \frac{k_z}{k_x} = \frac{5}{4}\mu\delta \tag{55}$$

During one period of oscillation, the sliding distance will be $4(A - A_c)$. The dissipated energy is equal to the work of the force of friction and is equal to

$$W = 4(A - A_c)\mu\delta \cdot k_z \tag{56}$$

Now let us apply this result to an oscillating contact of a parabolic indenter and a plane in the framework of the method of reduction of dimensionality, using the Eqs. (3), (4) and (10). The dissipation due to only one spring of the elastic foundation at the position x is equal to

$$\begin{aligned} \Delta W(x) &= 4\left(A - A_c(x)\right)\mu\delta(x) \cdot k_x \\ &= 4\mu E^* \left(A - \frac{5}{4}\mu\left(d - \frac{x^2}{R} \right) \right)\left(d - \frac{x^2}{R} \right)\Delta x \end{aligned} \tag{57}$$

Integrating over all gliding springs gives the dissipated energy

$$\begin{aligned} &W = 8E^* R^{1/2}\left(\frac{4}{5}\right)^{3/2} \mu^{-1/2} \cdot \\ &\left(A_{c0}(A - A_{c0})\left((A_{c0})^{1/2} - (A_{c0} - A)^{1/2} \right) + \frac{1}{3}(2A_{c0} - A) \right. \\ &\left. \left((A_{c0})^{3/2} - (A_{c0} - A)^{3/2} \right) - \frac{1}{5}\left((A_{c0})^{5/2} - (A_{c0} - A)^{5/2} \right) \right) \end{aligned} \tag{58}$$

For small amplitudes A, the dissipated energy can be developed in the Taylor series:

$$\begin{aligned} W = 8E^* R^{1/2}\left(\frac{4}{5}\right)^{3/2} \mu^{-1/2} A_{c0}^{5/2} \left(\frac{1}{12}\left(\frac{A}{A_{c0}} \right)^3 \right. \\ \left. + \frac{1}{48}\left(\frac{A}{A_{c0}} \right)^4 + \frac{3}{320}\left(\frac{A}{A_{c0}} \right)^5 \right) \end{aligned} \tag{59}$$

In particular, the first non-vanishing term gives

$$W \approx \frac{2}{3}\left(\frac{4}{5}\right)^2 E^* R^{1/2}\mu^{-1}d^{-1/2}A^3 \approx 0.42\cdot E^* R^{1/2}\mu^{-1}d^{-1/2}A^3 \tag{60}$$

For an arbitrary Poisson number, we would have

$$W \approx \frac{2}{3}\left(\frac{2(1-\nu)}{2-\nu}\right)^2 E^* R^{1/2}\mu^{-1}d^{-1/2}A^3 \tag{61}$$

which is exactly the 3D result obtained by Mindlin et al. [36].

8 Viscoelastic contacts and thermal effects

For viscoelastic bodies such as rubber, the contact can be seen as quasi-static when the penetration velocity and the sliding velocity are smaller than the smallest speed of sound (which corresponds to the smallest modulus of elasticity). If this condition is met and an area of an elastomer is excited at a frequency ω, then there is a linear relation between the force and displacement with stiffness that is proportional to the contact radius. Hence, this system can also be presented using a one-dimensional system, where the stiffness of the individual springs must be chosen according to (3). Rubber can be considered to be an incompressible medium so that $\nu = 1/2$ and for a contact between a rigid indenter and a rubber half-space, the stiffness must be chosen to be

$$\Delta k_z = E^*(\omega)\Delta x = \frac{E(\omega)}{1-\nu^2}\Delta x = \frac{2G(\omega)}{1-\nu}\Delta x = 4G(\omega)\Delta x \tag{62}$$

The corresponding relation for forces in the time domain reads

$$f_z(t) = 4\Delta x\int_{-\infty}^{t} G(t-t')\dot{z}(t')\mathrm{d}t' \tag{63}$$

Where $G(t)$ is the time dependent shear modulus [5].

For tangential contacts, the stiffness must be chosen according to Eq. (6):

$$\Delta k_x = G^*(\omega)\Delta x = \frac{4G(\omega)}{2-\nu}\Delta x \approx \frac{8}{3}G(\omega)\Delta x \tag{64}$$

The corresponding force relation in the time domain reads

$$f_x(t) = \frac{8}{3}\Delta x\int_{-\infty}^{t} G(t-t')\dot{z}(t')\mathrm{d}t' \tag{65}$$

The validity of the mapping of three-dimensional contacts onto a one-dimensional viscoelastic foundation is further based on the equivalence of surface profiles for all media with linear rheology at a given indentation. Let us illustrate this important topic by comparing the indentation of an elastic and a viscous medium. The surface profile is determined unambiguously by the equilibrium equation of the medium and the (linear) stress relation on the surface. For an elastic medium, the equilibrium relation reads

$$G\Delta\vec{u} + (\lambda + G)\nabla(\nabla\cdot\vec{u}) = 0 \tag{66}$$

where $\lambda = 2\nu G/(1-2\nu)$ is the first Lame-coefficient [37]. The corresponding "equilibrium equation" for a linearly viscous fluid is the Navier-Stokes equation without inertia terms [38]:

$$\eta\Delta\dot{\vec{u}} + (\xi + \eta)\nabla(\nabla\cdot\dot{\vec{u}}) = 0 \tag{67}$$

In the case of an elastic continuum, the stress is a linear function of the gradients of the displacement field $\vec{u}$, while in the case of a fluid, the same is valid for the gradient of the velocity field $\dot{\vec{u}}$. The same form of equations (after substitution of the displacement field with the velocity field) implies that all relations which are valid at a given contact configuration for an elastic continuum for force-displacement relations will be valid for a viscous medium for force-velocity relations. The incremental changes in contact configuration and indentation depth do not depend on elastic properties of the medium – this is seen very clearly in the fact, that the contact radius in the Hertz problem $a = \sqrt{Rd}$ does not depend on elastic moduli. This leads straightforwardly to the conclusion that at the given indentation depth, the configurations of an elastic and of a viscous medium are strictly identical. This is valid not only for rotationally symmetric profiles, but also for arbitrary profiles, however, only during the indentation phase. It was first Radok who found this property and used it for developing the contact mechanics of viscoelastic media [39].

Finally, let us note that the stationary equation of thermal conductivity

$$\Delta T = 0 \tag{68}$$

(Δ is the Laplace operator here and in Eqs. (66) and (67)) is of the same form as the equations of elasticity (66) and for fluid dynamics (67). The same is valid for equations of electrical conductivity. This leads to a close connection between the elastic properties and some electrical and thermal properties [8]. For example, the electrical contact conductance Λ is linearly proportional to the incremental stiffness: $k = \frac{\partial F_N}{\partial d} = E^* (\rho_1 + \rho_2)\Lambda/2$ [8], where ρ_1 and ρ_2 are the resistivities of the contacting bodies. Electrical and thermal properties can, therefore, be integrated into the method of reduction of dimensionality in a natural and simple way.

9 Normal contacts with rough surfaces

An important question is whether the method of reduction of dimensionality is restricted to the bodies of revolution or can be applied to a broader class of surface topographies, above all to that of the contact of rough surfaces. The importance of roughness was first stressed by Bowden and Tabor [1]. It was a hot topic in the 50s and 60s during the 20th century [2, 40] and remains an important research topic until now [41–46]. Numerical simulations of contacts between rough surfaces costs very much computation time and are one of the main reasons why numerical simulation methods are not used until now in engineering tribology. We will show below in this section that there are empirical and theoretical reasons to state that the method of reduction of dimensionality is applicable at least to randomly rough fractal surfaces as well, thus, providing a practical tool for the rapid simulation of contact problems. The validity of this hypothesis was first studied in Ref. [9]. However, from the present-day perspective, the results reported in Ref. [9] are only partially correct and must be generalized.

In order to cross over to a contact between bodies with rough surfaces, a rule for the production of a one-dimensional profile, which is equivalent to the three-dimensional body in a contact mechanical sense, must be formulated. As a motivation for this replacement, we use a few ideas from the model of Greenwood and Williamson [40]. The results and quality of the replacement system, however, prove to be more general than the Greenwood-Williamson model. In particular, the method of reduction of dimensionality allows contacts from the limit of very small forces to the complete contact to be modeled.

In the model of Greenwood and Williamson, the individual contacts are considered to be independent from each other. Under these conditions, only the distribution of the heights of the asperities and the radii of curvature play a role. So, our goal is first to generate a one-dimensional system, which has the necessary statistical distributions of heights and radii of curvature. To simplify matters, we assume that the topographies of both the two-dimensional surface (of a three-dimensional body) and of its one-dimensional mapping can be unambiguously characterized by their *power spectra* $C_{2D}(\vec{q})$ and $C_{1D}(\vec{q})$, which are defined according to

$$\begin{aligned} C_{2D}(\vec{q}) &= \frac{1}{(2\pi)^2}\int \left\langle h(\vec{x})h(\vec{0})\right\rangle e^{-i\vec{q}\cdot\vec{x}}\mathrm{d}^2x, \quad \text{for a surface} \\ C_{1D}(q) &= \frac{1}{2\pi}\int \left\langle h(x)h(0)\right\rangle e^{-iqx}\mathrm{d}x, \qquad \text{for a line} \end{aligned} \tag{69}$$

where $h(\vec{x})$ is the height profile taken from the average so that $\langle h\rangle = 0$; $\langle . \rangle$ means averaging over the statistical ensemble. Furthermore, we assume that the surface topography is statistically homogeneous and isotropic. Under these conditions, the power spectrum $C_{2D}(\vec{q})$ is only dependent on the magnitude q of the wave vector $\vec{q}$.

Many technically relevant surfaces are fractal self-affine surfaces [4]. These surfaces have a spectral density obeying a power law:

$$\begin{aligned} C_{2D}(q) &= \text{const}\cdot\left(\frac{q}{q_0}\right)^{-2H-2}, \quad \text{for a surface} \\ C_{1D}(q) &= \text{const}\cdot\left(\frac{q}{q_0}\right)^{-2H-1}, \quad \text{for a line} \end{aligned} \tag{70}$$

where H is the Hurst exponent ranging from 0 to 1 [4]. It is directly related to the fractal dimension of an original two-dimensional surface $D_f = 3 - H$.

The surface topography is calculated with the help of the power spectrum according to

$$h(\vec{x}) = \sum_{\vec{q}} B_{2D}(\vec{q}) \exp\left(i\left(\vec{q}\cdot\vec{x} + \phi(\vec{q})\right)\right)$$
$$B_{2D}(\vec{q}) = \frac{2\pi}{L}\sqrt{C_{2D}(\vec{q})} = \overline{B}_{2D}(-\vec{q}) \tag{71}$$

for two-dimensional surfaces and with

$$h(x) = \sum_{q} B_{1D}(q) \exp\left(i\left(qx + \phi(q)\right)\right)$$
$$B_{1D}(q) = \sqrt{\frac{2\pi}{L} C_{1D}(q)} = \overline{B}_{1D}(-q) \tag{72}$$

for one-dimensional lines, with random phases $\phi(\vec{q}) = -\phi(-\vec{q})$ on the interval $[0, 2\pi)$.

In order to produce a one-dimensional system with the same contact properties as the three-dimensional system, the following rule for generating the one-dimensional power spectrum was proposed in Ref. [9]:

$$C_{1D}(q) = \pi q C_{2D}(q) \tag{73}$$

Qualitative arguments for this rule are the following: The averages of the squares of the heights for the two-dimensional and one-dimensional cases, respectively, are

$$\langle h^2 \rangle_{2D} = 2\pi \int_0^\infty q C_{2D}(q)\,\mathrm{d}q \tag{74}$$

and

$$\langle h^2 \rangle_{1D} = 2 \int_0^\infty C_{1D}(q)\,\mathrm{d}q \tag{75}$$

They are the same when $C_{1D}(q) = \pi q C_{2D}(q)$. The corresponding root mean squares of the surface gradient $\langle \nabla z^2 \rangle$ and curvature $\langle \kappa^2 \rangle$ also coincide in this case (For two-dimensional cases, we define $\kappa^2 = \kappa^{(1)}\kappa^{(2)}$, where $\kappa^{(1)}$ and $\kappa^{(2)}$ are the principal radii of curvature of the surface.). Note that the Hurst exponents of both one- and two-dimensional surfaces coincide as well. This last property is very important and allows an analytical substantiation for the applicability of the method of reduction of dimensionality to randomly rough surfaces to be given. From our present point of view, Eq. (73) must be replaced by a more general relation:

$$C_{1D}(q) = \lambda(H) q C_{2D}(q) \tag{76}$$

where $\lambda(H)$ is a coefficient which depends on the Hurst exponent (see details below in this section).

Let us illustrate the applicability of the method of reduction of dimensionality using the example of normal stiffness of bodies with rough surfaces. Stiffness of fractally rough surfaces without long wavelength cut-off has been investigated in Ref. [45]. Consider a cylindrical rigid indenter with diameter $L = 2a$, having a self-affine fractal surface described by Eq. (70). If it is pressed into an elastic half-space, first the tallest peak comes into contact and finally, at a very large normal force, complete contact will be achieved. In this final state, the contact stiffness is equal to $k_{z,\max} = E^* L$. Now, we use the Eq. (76) of the surface power spectrum and generate a rough line according to Eq. (72), having the length L. This choice of length guarantees automatically that the maximum stiffness at the complete contact will exactly coincide for three- and one-dimensional cases. Furthermore, we concentrate our attention to the region of small forces and incomplete contact. It was shown in Ref. [45] that there are several rigorous scaling relations which the dependence of contact stiffness k_N and the normal force must fulfill. These scaling relations lead to the following general form of the stiffness-force dependence, both for the one- and three-dimensional case:

$$\frac{k_N}{E^* L} = \zeta \left(\frac{F}{E^* h L}\right)^{\alpha} \tag{77}$$

where α is a constant exponent and ζ is a constant coefficient; both of them may only depend on the Hurst exponent.

There are analytical considerations supporting the power law dependence of the contact stiffness and the strict equivalence of three-dimensional and one-dimensional results for small fractal dimensions [46]. For fractal surfaces without long wavelength cut-off, the surface has a pronounced non-planarity on the largest scale. Therefore, the contact at small contact forces is localized in the vicinity of only one point of apparent contact area. Now, let us make the

following transformation of the surface:

$$\begin{aligned} L' &= CL \\ h' &= C^H h \\ d' &= d \end{aligned} \tag{78}$$

According to the definition of a self-affine surface, this transformation provides the same surface (or a surface with the same statistical properties) as long as the real contact spot is inside the initial size of the system. This means that Eq. (78) lets the complete "contact state," including the contact force and contact stiffness (defined as $\partial F / \partial d$), remain unchanged:

$$\begin{aligned} F' &= F \\ k' &= k \end{aligned} \tag{79}$$

Substitution of the Eqs. (78) and (79) into (77) gives

$$\alpha = \frac{1}{1+H} \tag{80}$$

These arguments do not depend on the dimensionality of the system and are valid for both the initial three-dimensional contact and its one-dimensional mapping. The constants ζ may, of course, be different, but can easily be adjusted — just as in the case of simple rotationally of symmetric bodies — with a universal scaling factor, which depends only on the Hurst exponent and must be determined once empirically with large-scale direct simulations. This has already been done in Ref. [46].

MRD, thus, produces correct asymptotic dependences of the contact stiffness of self-affine fractal surfaces as well — both in the limit of very small and very large loads. Comparisons of the statistical scattering of contact properties depending on particular realization also coincide in both cases, which gives the possibility of applying the method of reduction of dimensionality to the study of fluctuation of contact properties (e.g., in the problem of rolling noise [20]).

Self-affine surfaces are often investigated in the range of $0 < H < 1$, but Eq. (70) does not naturally impose such a restriction. In Ref. [48], the contact stiffness was investigated in the range of Hurst exponents from $H = -1$ to $H = 3$. In each case, the contact stiffness was found to rise with the force according to a power law, Eq. (77). The values of the exponent α found from direct 3D simulations are shown in Fig. 6 by blue crosses. What could be mistaken as a fitting curve of the 3D results in Fig. 6 is actually the independent raw data from the simulations with the method of reduction of dimensionality (red line).

So far, we considered fractal surfaces without roll-off. However, the results of surfaces with roll-off are effectively included in the picture shown in Fig. 6. Indeed, a spectral density with a broad roll-off region (constant power density) corresponds formally to $H = -1$, which is the left uppermost point in the range of Hurst exponents investigated here.

The conversion factor $\lambda(H)$ in Eq. (76) depends generally on the Hurst Exponent. The dependence of $\lambda(H)$ on the Hurst Exponent implies that the general rule for any spectral density (not only the self-affine type) will be an integral transformation of the form

$$C_{1D}(q) = \int_q^\infty C_{2D}(q')K(q,q')\mathrm{d}q' \tag{81}$$

Where $K(q,q')$ is a homogeneous function of arguments q and q' of zero order. The exact form of this integral transformation is not yet known.

Until now, we considered randomly rough surfaces, which are flat at the average. It was shown in Ref. [48]

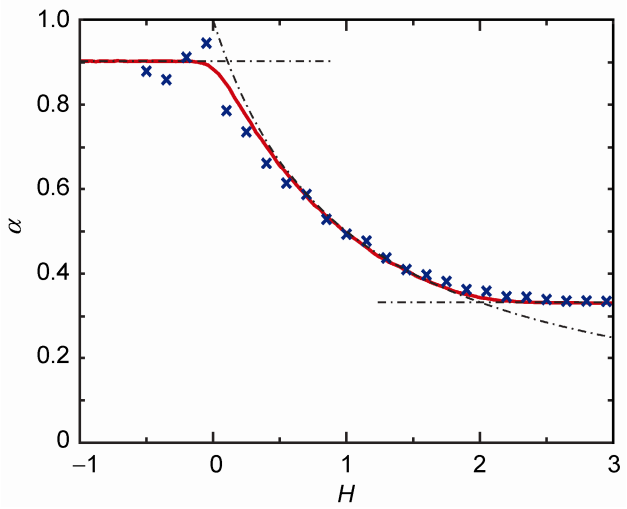

Fig. 6 The exponent α from Eq. (77) as a function of the Hurst Exponent of a rough surface. The blue crosses are the results of 3D boundary element simulations; the red line was obtained using the method of reduction of dimensionality. (Source: Ref. [49])

that the method of reduction of dimensionality is also applicable to combined profiles (e.g., a rough parabolic indenter).

10 Force of friction

10.1 Sliding friction force between an elastomer and a rigid rough surface

Friction between rough solid surfaces is of considerable importance in many applications. In the present paper we confine ourselves only to the consideration of friction between a rigid rough surface and an elastomer with linear rheology. We do not consider adhesion, which can also contribute to friction [50]. As discussed above, the force-displacement relations in this case are described correctly by the method of reduction of dimensionality. We will illustrate this with two examples. Grosch first established that the friction of elastomers is determined by the internal losses in contacting bodies and is, hence, closely related to the rheology of these materials [51]. Simple analytical estimations [5] show that the coefficient of friction between an elastomer and a rough solid surface obeys the following relation:

$$\mu = \xi \nabla z \frac{G''(kv)}{\left|\hat{G}(kv)\right|} \tag{82}$$

Where ∇z is the mean square slope (gradient) of the solid surface profile $z = z(x, y)$, $\hat{G}(\omega)$ is the frequency dependent complex shear modulus of the elastomer, $G''(\omega)$ is the imaginary part of this complex quantity, k is the characteristic wave vector of the solid surface profile, v is the relative velocity of sliding, ξ is a dimensionless constant on the order of unity, and $\left|\hat{G}(\omega)\right|$ is the modulus of the complex shear modulus. Since Eq. (82) is derived on the basis of qualitative considerations, the exact value of a constant ξ is unknown and can only be determined by means of numerical simulations.

Eq. (82) acquires a simpler form, provided that the complex shear modulus is purely imaginary (or its imaginary part is much greater than the real part). Then, the ratio $\frac{G''(\omega)}{\left|\hat{G}(\omega)\right|}$ is unity and Eq. (82) reduces to

$$\mu = \xi \nabla z \tag{83}$$

In Ref. [12], it was proven by direct numerical simulation that this relation is valid for fractal surfaces with the coefficient ξ being approximately 1.

The more general Eq. (82) was validated in Refs. [13] and [16]. There, the time dependent modulus of the form

$$G(t) = G_0 + G_1 \tau_1 \int_{\tau_1}^{\tau_2} \tau^{-s} e^{-t/\tau} \mathrm{d}\tau \tag{84}$$

has been used with $G_0 = 1$ MPa, $G_1 = 1000$ MPa, $\tau_1 = 10^{-2}$ s, $\tau_2 = 10^2$ s, and $s = 2$. This dependency is characterized by a broad spectrum of relaxation times ranging from 10^{-2} s to 10^2 s. The results of numerical simulation using Eq. (63) is presented together with the analytical estimation Eq. (82) in Fig. 7. One can see that the numerical simulation reproduces the three-dimensional estimation very well. However, as there are no exact three-dimensional calculations for the force of friction, it is not possible to decide if the small discrepancy is due to the inaccuracy in the one-dimensional numerical simulation or to the inaccuracy in the three-dimensional estimation.

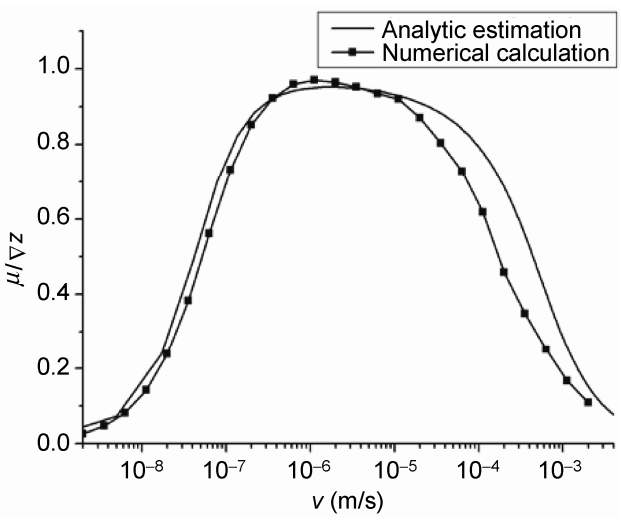

Fig. 7 Dependence of the friction coefficient for a contact of a two-dimensional rough, non-fractal surface with a half-space exhibiting the linear rheological law Eq. (84). The solid line is estimation Eq. (82) and the dots, the numerical simulation using the method of reduction of dimensionality.

10.2 Dependence of the static friction force on the normal force

Amonton's law for dry friction (proportionality of the force of friction to the normal force) is known to be only a first rough approximation. The more detailed models for the dry friction force are of very high scientific and technical importance. In this section we illustrate an approach to this problem based on the method of reduction of dimensionality. The results of this section follow Ref. [14]. Imagine, for example, a viscoelastic body which is characterized by some elasticity and viscosity. If a rigid rough body is pressed onto such a body and is held under this force for a long time, then the contact configuration will only depend on the elastic modulus of the medium. If the body is now moved rapidly in the tangential direction, then it will react as a viscous body and the instantaneous coefficient of friction will be just of the order of magnitude of the instant rms value of the surface slope [5]. This consideration shows that a correlation must exist between the coefficient of friction and the true instant rms value of the surface slope. In the following we investigate the dependence of the average slope in the contact region of an elastic continuum and a rough rigid body. It will give us, at least qualitatively, the dependence of the static friction force between a rigid body and an elastomer on the normal force. As many technical surfaces of interest are self-affine fractal surfaces, we will investigate this class of rough surfaces. In Ref. [14], an elastomer block of a length L was considered. One dimensional rough lines were produced according to the rule Eq. (72) with a power spectrum Eq. (70). The summation in Eq. (72) was over the wave vectors in the interval

$$\frac{\pi}{L} < |q| < \frac{1}{10}\frac{\pi}{\Delta x} \tag{85}$$

where $N = L/\Delta x$ is the total number of discretization points. The relation Eq. (85) means that there is no cut-off wave vector at the lower limit of the interval apart from the natural cut-off due to the finite size of the system. On the other side, at the upper limit there is a cutoff wave vector which guarantees that the line is smooth enough even at the smallest scale. This profile is brought into contact with the above defined elastic foundation and pressed with the total normal force F (see Fig. 8).

After the penetration depth has been acquired numerically for a given normal force, the mean slope of the single line in places of contact was calculated:

$$\nabla z_{\text{cont}} \equiv \sqrt{\left\langle \left(\frac{z(x_{i+1}) - z(x_i)}{\Delta x} \right)^2 \right\rangle}, \quad \text{only for points in contact} \tag{86}$$

The rms gradient found in this way was averaged over 300 realizations of the rough line with the same spectral density. To characterize the surface, the rms value of the height distribution

$$h = \sqrt{\langle z(x)^2 \rangle} \tag{87}$$

and the rms value of the surface gradient over the whole system

$$\nabla z = \sqrt{\langle (\partial z / \partial x)^2 \rangle} \tag{88}$$

were introduced.

There are several strict scaling relations which must be fulfilled independent of the particular form of the spectral density. If the rms value of the height

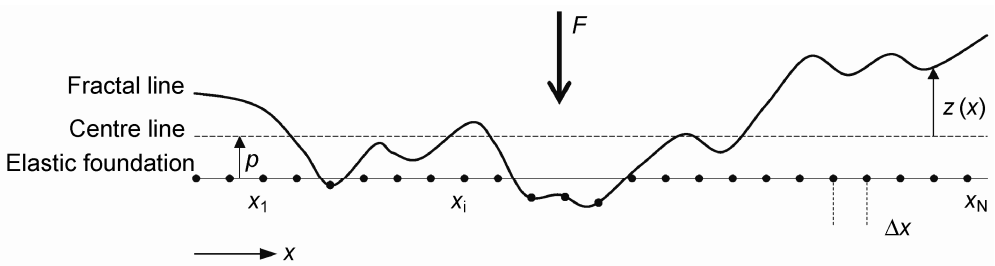

Fig. 8 Fractal line in contact with discretized elastic foundation.

distribution as well as the indentation depth is increased by some factor, both gradients (86) and (88) as well as the normal force will increase by the same factor. For the given contact configuration, the force must be proportional to the elastic modulus. We fulfill both requirements if we introduce the dimensionless variables

$$\xi = \frac{\nabla z_{\text{cont}}}{\nabla z} \tag{89}$$

$$f = \frac{F}{E^* hL} \tag{90}$$

and search for a function $\xi(f)$.

One example of the numerical simulation is shown in Fig. 9.

For the most typical values of H around 0.7, the following relation has been derived:

$$\xi = a + b\ln(f) \tag{91}$$

with $a \approx 2.9$ and $b \approx 0.14$. Thus, the dependence of the rms gradient value on the force can be written as

$$\frac{\nabla z_{\text{cont}}}{\nabla z} = 2.9 + 0.14 \cdot \ln\left(\frac{F}{E^* hL}\right) \tag{92}$$

Increasing the force by a factor of 500 changes the rms gradient (and, therefore, the coefficient of friction) by a factor of 3 to 4. This is in accordance with the strong dependence of the coefficient of friction on the normal force observed in many experiments (see, for example, Ref. [52]). According to the method of

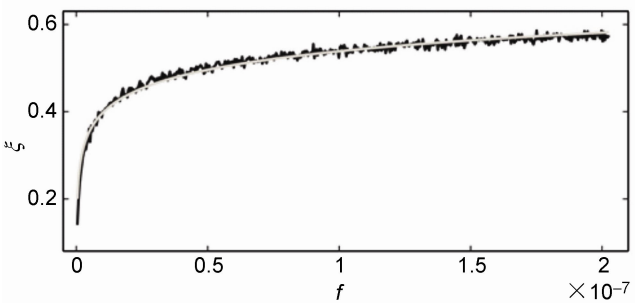

Fig. 9 Dependence of the dimensionless mean slope in contact on the dimensionless normal force. Curves are shown for $N = 10^5$, $L = 10^5$, $H = 1$, $E^* = 1$ and number of realizations $t = 300$. The force F goes from 1 to 500. For $F = 500$, the average number of points in contact is 40. The simulation returns $a = 1.5289$ and $b = 0.0614$ for the natural logarithmic fit (gray line).

reduction of dimensionality, these results should be valid for three-dimensional systems as well, provided the length of the system is replaced by $L = 2\sqrt{A}/\sqrt{\pi}$, where A is the apparent area of contact:

$$\frac{\nabla z_{\text{cont}}}{\nabla z} \approx 2.9 + 0.14 \cdot \ln\left(\frac{\sqrt{\pi} F}{2E^* h\sqrt{A}}\right) \tag{93}$$

This relation shows that the coefficient of friction has only weak, logarithmic dependence on the argument $\frac{\sqrt{\pi} F}{2E^* h\sqrt{A}}$. This is the reason, why it can be considered, in a first approximation, to be a constant. In the higher approximation, however, it depends on the normal force, the apparent contact area A, the roughness, and the material properties (e.g., E^*).

11 Objections to the method of reduction of dimensionality and its area of application

First, we remember that MRD in the present formulation is only applicable to systems with linear rheology. Furthermore, it is only valid in the half-space approximation just as the majority of results in contact mechanics obtained so far. The possibilities of extending the method to non-linear (including elastoplastic) contacts by applying the method in the incremental form have not yet been studied.

It must be stressed that the equivalence of the contact properties of a true 3D system and its 1D substitute in the method of reduction of dimensionality does not relate to all properties of the contact but only to its macroscopic response to external forces. MRD can be applied if the macroscopic contact forces are of interest. Many such situations are described in Ref. [53]. That the force-displacement relations are described correctly by the reduction method has been proven (either analytically or by numerical simulations) for any sort of self-affine surfaces (both in the form of single contacts or randomly rough surfaces) and can be considered now as a solid foundation of the method. Furthermore, in the case of axis-symmetric surfaces, the method is true for non-self-affine surfaces, and we hope that this will be the case for any randomly rough surfaces as well.

Surely, there are many properties which cannot be described in the framework of the method of reduction of dimensionality, for example, spatial correlation functions of stresses or displacements. In many cases, however, we are interested not in the detailed spatial distribution of forces but only in the macroscopic response of a system. This is by no means a new concept but rather the usual direction in which physics is going in description of macroscopic systems. Thus, we use the notion of the pressure of a gas if we are not interested in the true (and extremely nonhomogeneous, both temporarily and spatially) structure of forces caused by molecular impacts. The same is true for the contact mechanics, where the macroscopic force-displacement response delivers the most important information, which is needed for engineering applications. The force-displacement relations determine the contact stiffness and, in this way, the dynamic properties of a tribological system; they determine the statistical properties of the contact forces and, thus, the noise due to rolling or sliding; they determine the work done by the external forces and, thus, the frictional forces and damping; they determine the thermal production, conduction, and electrical conductivity. Outside the realm of the macroscopic reaction to the force action, the method of reduction of dimensionality generally cannot be applied.

An exception when much more detailed information can be obtained in the framework of the reduction method, is that of axis-symmetric contacts. In the case of single axially-symmetric contacts, the method can also be used for calculation of the contact area and the stress distribution in the area of real contact. This is, however, not true for randomly rough surfaces. In Ref. [9], the simple transformation rule Eq. (73) has been suggested and it was claimed that it is possible to correctly determine the contact area from the 1D simulations. From the present point of view, the transformation Eq. (73) is not completely correct; the coefficient in this equation is in reality not equal to π but depends on the Hurst exponent. The claim to correctly describe the contact is also not completely correct. While the initial linear asymptote in the dependence of the contact area on normal force is described correctly, it becomes rapidly incorrect at larger forces. That the contact area and the contact stiffness cannot be both described correctly by the reduction method follows immediately from the well-known property that the saturation value of the contact stiffness is achieved in macroscopic systems much earlier than the complete material contact [5]. In Ref. [9], the size of the system was accidentally chosen in such a way that the area-force dependence was correct up to relatively large contact. This result, however, cannot be generalized.

The main objection to MRD, which is repeated again and again over years, is that the 1D substitute system has no interrelations between springs of the elastic foundation and, thus, cannot describe the 3D original having such correlations. This objection is based on the errant mental image of the 1D substitute system as a sort of a spatial cross-section of the 3D topography. In reality, the 1D system is not a cross-section; it has another dimension and topology. The neighboring points of the 3D system cannot be identified in the 1D substitute system, and thus, the elastic coupling loses its sense. The 1D system must rather be considered as an abstract model, which has no immediate intuitive interrelation with the original 3D system. In MRD, we are only interested in the macroscopic response of the system. There is no mathematical theorem preventing a "partial equivalence in the sense of forces" of a 3D system with elastic coupling and a 1D system without such coupling. This can be seen already from the scaling considerations leading to the conclusion of equivalence. The incorrectness of the "no-coupling-argument" follows immediately from the exactness of the method of reduction of dimensionality when applied to the axisymmetric bodies. For these bodies, the same is valid as for any arbitrary contact: the 3D system has spatial correlations and the 1D does not. This, however, does not prevent the method of being applicable to this class of contacts. Obviously, the elastic coupling of the 3D system is correctly taken into account by both the changed dimensionality and the modified indenter profile.

12 Discussion

The described method of reduction of dimensionality maps a three-dimensional contact problem to one of

one dimension. This leads to a drastic reduction in the computation time and trivialization of analytical calculations. The reduction which is achieved by this method is two-fold: First, a system, whose degrees of freedom correspond to a three-dimensional space, is replaced by a system with the same linear size, whose degrees of freedom correspond to a one-dimensional space. The second, equally important reduction is that a system with interacting degrees of freedom is replaced by a system with independent degrees of freedom. This property opens the possibility of further reduction of calculation time by parallel processing of independent degrees of freedom. A possibility of such replacement seems at first glance miraculous, but was rigorously proved for at least two classes of surface topographies: (a) for arbitrary bodies of revolution and (b) for randomly rough fractal self-affine surfaces. The mapping is no approximation, but is exact. The time reduction for realistic systems of technical interest is at least six decimal orders of magnitude, thus, opening completely new possibilities in numerical simulation of contacts with real topography. In particular, it becomes possible to incorporate the microscopic simulations directly (in each time step) into a macroscopic simulation of the system dynamics and, thus, really close the gap between the micro- and macro-world for many classes of tribological problems.

Table 1 summarizes the rules of the method of reduction of dimensionality. The horizontal arrows show the rules for the replacement of axisymmetric contacts by one-dimensional single contacts and of rough surfaces by one-dimensional "rough lines." It is interesting to note that a further reduction is possible. As the force-displacement relations for the randomly rough self-affine surfaces and axisymmetric profiles with the same Hurst-Exponent ($H = n$) are described by power-laws with the same power, displacement of fractal surfaces by simple rotationally symmetric profiles is possible, as long as we are only interested in the ensemble averaged dependencies. This reduction is shown in Table 1 by dashed arrows. It is described in more detail in the book [48].

Coming back to the problem of linking the scales in contact and friction mechanics, we would like

Table 1 Equivalences and transformation rules of the method of reduction of dimensionality.

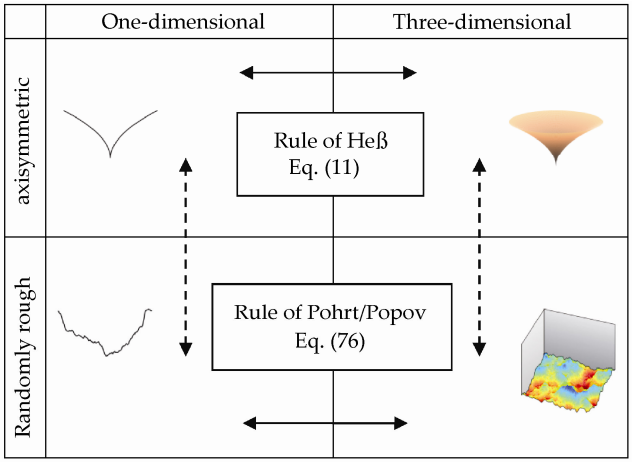

to illustrate the place of the method of reduction of dimensionality by means of the schemes shown in Fig. 10 and Fig. 11 [54]. It is important to stress that the power spectrum of typical surfaces has no gaps in the wave vector space. This means that a clear separation of "macroscopic" and "microscopic" scales is principally impossible for frictional systems and the separation is always more or less arbitrary. A typical "engineering approach" (Fig. 10a) is to choose the wave vector separating the "macroscopic" and "microscopic" scales just at the scale of the system as a whole. The macroscopic scale is then described explicitly with certain "one-scale" methods, such as finite elements. The entirety of the rest of the system dynamics is not described explicitly. Instead, one attempts to describe this part of the system dynamics with a proper "law of friction." It is no wonder that this "law of friction" is highly system dependent. On the other hand, very many attempts have been made to calculate the force of friction starting from some "microscopic" model. The authors of such theories choose a scale that they consider to be the most important for the system considered and calculate the dynamics explicitly on this scale. The result is a contribution to friction stemming from the chosen scale (Fig. 10b). Even if such an approach may allow for a qualitative understanding of friction at the chosen scale, it will never have quantitative predictive power. Finally, there are many scientists studying the frictional forces at the molecular scale (Fig. 10c), omitting all intermediate scales.

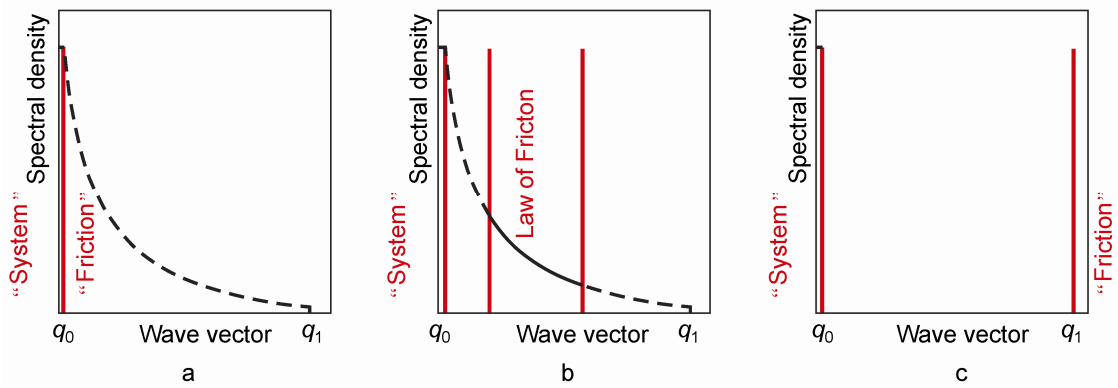

Fig. 10 Typical paradigms in the physics of friction: (a) "The world of an engineer" — the scale separation occurs immediately at the largest scale of the system as a whole. (b) "The world of a friction physicist" — only one intermediate scale is chosen and is simulated. (c) "The world of a molecular physicist" — only the molecular level is considered.

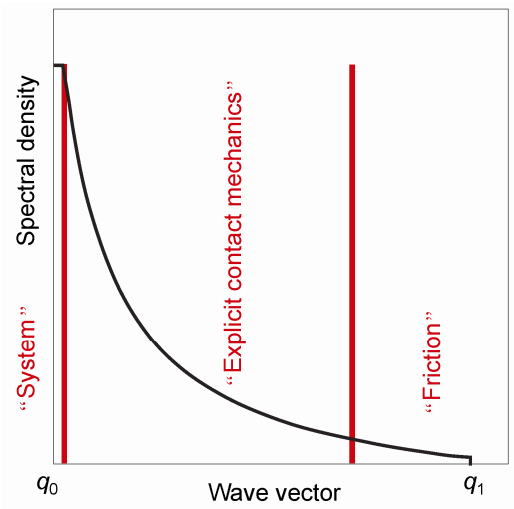

Fig. 11 "Filling in the gap" between "macro" and "micro".

One of the possibilities to "fill in the gap" between the "macro scale" and the "micro scale" (between q_0 and q_1 in Fig. 10c) is illustrated in Fig. 11. The strategy shown in this figure is to define three scale intervals: the macroscopic scale of the system as a whole (characterized by the wave vector q_0) is still the scale which must be explicitly simulated. On the other hand, we define a much smaller "microscopic scale" (characterized by the wave vector q_1), which we cannot describe explicitly due to some reasons (lack of material parameters, surfaces parameters, and so on). The contribution from the smallest scale is considered to be "friction at the microscopic scale." For this friction, an empirically measured or numerically motivated "law of friction" is needed. The scales between these limits must be treated with an explicit contact mechanical method which accepts the loss of information about parts of the system but allows for a small number of especially meaningful macroscopic quantities to be calculated *fast*. In the field of contact mechanics for real surfaces, one such possibility is the method of reduction of dimensionality.

The applicability of the method of reduction of dimensionality is, of course, restricted to the scales where macroscopic continuum mechanics can be used. This means that the smallest, atomic scale cannot be incorporated into the method directly. However, as already mentioned above, it is possible to summarize the interactions on the smallest scale to a phenomenological friction, which must be introduced additionally as an empirical frictional law. In Ref. [55], it was shown that the boundary between macro- and micro-description can be shifted continuously in a sort of renormalization group, which gives different laws of friction at different scales. What the method of reduction of dimensionality really does is shifting this boundary between micro and macro to the smallest possible scale, at which a mechanical description of a material fails. It is interesting to analyze whether it is principally possible to introduce interactions of the type of the Prandtl-Tomlinson model [56] or its extensions for boundary lubrication [57] on the smallest scale, thus, providing a link between macroscopic tribology and atomic scale tribology [58]. All of these topics are matters for future research.

As proposed already in the Ph.D thesis by T. Geike, other reduction methods are also possible. For example, some equivalences can be found by replacing a three dimensional contact by a contact with a homogeneous 2D medium or a 2D medium, which Young modulus is an arbitrary power function of the depth [59]. A more detailed analysis of such "partial" reduction methods has been done for arbitrary bodies of revolution in Ref. [21] and for randomly rough surfaces in a recent paper [60].

Acknowledgement

I am grateful to my colleagues and guests at the Berlin University of Technology J. Benad, A. Dimaki, A.E. Filippov, T. Geike, R. Heise, M. Heß, S. Kürschner, Q. Li, R. Pohrt, M. Popov, S.G. Psakhie, J. Starcevic, E. Teidelt, R. Wetter, E. Willert for many valuable discussions of the fundamentals of the method of reduction of dimensionality and its extensions. I thank R. Pohrt for providing not yet published results and permission to use them in this review. I acknowledge the useful critical remarks by B.N.J. Persson and M. Müser, which contributed to the understanding of the region of applicability of the method. I acknowledge financial support of this research by the Deutsche Forschungsgemeinschaft (DFG) and the Deutscher Akademischer Austausch Dienst (DAAD) in the framework of several projects.

References

[1] Bowden F P, Tabor D. *The Friction and Lubrication of Solids*. Oxford: Clarendon Press, 1986.

[2] Archard J F. Elastic deformation and the laws of friction. *Proc R Soc A* **243**: 190−205 (1957)

[3] Archard J F. Contact and rubbing of flat surfaces. *J of Appl Phys* **24**: 981−988 (1953)

[4] Persson B N J. Contact mechanics for randomly rough surfaces. *Surf Sci Rep* **61**: 201-227 (2006)

[5] Popov V L. Contact Mechanics and Friction: Physical Principles and Applications. Berlin: Springer-Verlag, 2010.

[6] German-Russian Workshop on "Numerical simulation method in tribology: possibilities and limitations", TU Berlin, March 14–17, 2005. Contributions published in the special issue of "Tribology International", (*Trib Int*, **40**, No. 6, Guest editors Popov V and Ostermeyer G-P).

[7] Popov V L, Psakhie S G. Numerical simulation methods in tribology. *Tribology International* **40**: 916–923 (2007)

[8] Barber J R. Bounds on the electrical resistance between contacting elastic rough bodies. *Proc R Soc Lond A* **495**: 53−66 (2003)

[9] Geike T, Popov V L. Mapping of three-dimensional contact problems into one dimension. *Phys Rev E* **76**: 036710 (2007)

[10] Geike T, Popov V L. Reduction of three-dimensional contact problems to one-dimensional ones. *Tribology International* **40**: 924−929 (2007)

[11] Kürschner S, Filippov A E. Normal contact between a rigid surface and a viscous body: Verification of the method of reduction of dimensionality for viscous media. P*hys Mesomech* **15**: 270−274 (2012)

[12] Popov V L, Filippov A E. Force of friction between fractal rough surface and elastomer. *Tech Phys Lett* **36**: 525−527 (2010)

[13] Popov V L, Dimaki A. Using hierarchical memory to calculate friction force between fractal rough solid surface and elastomer with arbitrary linear rheological properties. *Tech Phys Lett* **37**: 8−11 (2011)

[14] Benad J. On the dependence of the static friction force between a rigid, randomly rough fractal surface and a viscoelastic body on the normal force. *Phys Mesomech* **15**: 300−302 (2012)

[15] Li Q. Dependence of the kinetic force of friction between a randomly rough surface and simple elastomer on the normal force. *Phys Mesomech* **15**: 303−305 (2012)

[16] Heise R. Multiscale simulation of friction with normal oscillations in the method of reduction of dimensionality. *Phys Mesomech* **15**: 316−318 (2012)

[17] Teidelt E, Willert E, Filippov A E, Popov V L. Modeling of the dynamic contact in stick-slip microdrives using the method of reduction of dimensionality. *Phys Mesomech* **15**: 287−292 (2012)

[18] Stracevic J, Filippov A E. Simulation of the influence of ultrasonic in-plane oscillations on dry friction accounting for stick and creep. *Phys Mesomech* **15**: 330−332 (2012)

[19] Wetter R. Shakedown and induced microslip of an oscillating frictional contact. *Phys Mesomech* **15**: 293−299 (2012)

[20] Popov M. Contact force resulting from rolling on a self-affine fractal rough surface. *Phys Mesomech* **15**: 342−344 (2012)

[21] Heß M. *Über die Abbildung ausgewählter dreidimensionaler Kontakte auf Systeme mit niedrigerer räumlicher Dimension*. Göttingen: Cuvillier-Verlag, 2011.

[22] Heß M. On the reduction method of dimensionality: The exact mapping of axisymmetric contact problems with and without adhesion. *Phys Mesomech* **15**: 264−269 (2012)

[23] Johnson K L. *Contact Mechanics*. Cambridge: Cambridge University Press, 1987.
[24] Sneddon I N. The relation between load and penetration in the axisymmetric boussinesq problem for a punch of arbitraryprofile. *Int J Eng Sci* **3**: 47–57 (1965)
[25] Ejike U B C O. The stress on an elastic half-space due to sectionally smooth-ended punch. *Journal of Elasticity* **11**: 395−402 (1981)
[26] Griffith A A. The phenomena of rupture and flow in solids. *Phil Trans R Soc Lond A* **221**: 163–198 (1921)
[27] Johnson K L, Kendall K, Roberts A D. Surface energy and the contact of elastic solids. *Proc R Soc A* **324**: 301–313 (1971)
[28] Popov V L. *Kontaktmechanik und Reibung: Von der Nanotribologie bis zur Erdbebendynamik.* Berlin: Springer, 2010.
[29] Prandtl L. Ein Gedankenmodell für den Zerreißvorgang spröder Körper. *ZAMM* **13**: 129–133 (1933)
[30] Maugis D. *Contact, Adhesion, and Rupture of Elastic Solids*. Berlin: Springer Verlag, 2000.
[31] Popov V L. Basic ideas and applications of the method of reduction of dimensionality in contact mechanics. *Physical Mesomechanics* **15**: 254−263 (2012)
[32] Popov V L, Filippov A E. Adhesive properties of contacts between elastic bodies with randomly rough self-affine surfaces: A simulation with the method of reduction of dimensionality. *Phys Mesomech* **15**: 324−329 (2012)
[33] Cattaneo C. Sul contatto di due corpi elastici: distribuzione locale degli sforzi. *Rendiconti dell'Accademia nazionale dei Lincei* **27**: 342−348, 434−436, 474−478 (1938)
[34] Mindlin R D. Compliance of elastic bodies in contact. *Journal of Applied Mechanics* **16**: 259–268 (1949)
[35] Jäger J. Axi-symmetric bodies of equal material in contact under torsion or shift. *Archive of Applied Mechanics* **65**: 478−487 (1995)
[36] Mindlin R D, Mason W P, Osmer J F, Deresiewicz H. Effects of an oscillation tangential force on the contact surfaces of elastic spheres. *Pros.1st US National Congress of Applied Mechanics:* 203–226 (1952)
[37] Landau L D, Lifschitz E M. *Lehrbuch der Theoretischen Physik, Band 7: Elastizitätstheorie*. Berlin: Akademie-Verlag, 1965.
[38] Landau L D, Lifschitz E M. *Lehrbuch der Theoretischen Physik, Band 6: Hydrodynamik*. Berlin: Akademie-Verlag, 1991.
[39] Radok J R M. Viscoelastic stress analysis. *Q Appl Math* **15**: 198−202 (1957)
[40] Greenwood J A, Williamson J B P. Contact of nominally flat surfaces. *Proc R Soc A* **295**: 300−319 (1966)
[41] Hyun S, Robbins M O. Elastic contact between rough surfaces: Effect of roughness at large and small wavelengths. *Tribol Intern* **40**: 1413−1422 (2007)
[42] Campana C, Müser M H. Practical Green's function approach to the simulation of elastic semi-infinite solids. *Phys Rev B* **74**: 075420 (2006)
[43] Akarapu S, Sharp T, Robbins M O. Stiffness of contacts between rough surfaces. *Phys Rev Lett* **106**: 204301 (2011)
[44] Campana C, Persson B N J., Müser M H. Transverse and normal interfacial stiffness of solids with randomly rough surfaces. *J Phys: Condens Matter* **23**: 085001 (2011)
[45] Pohrt R, Popov V L. Normal contact stiffness of elastic solids with fractal rough surfaces. *Phys Rev Lett* **108**: 104301 (2012)
[46] Pohrt R, Popov V L, Filippov A E. Normal contact stiffness of elastic solids with fractal rough surfaces for one- and three-dimensional systems. *Phys Rev E* **86**: 026710 (2012)
[47] Pohrt R, Popov V L. Contact mechanics of randomly rough self-affine surfaces. *Tribology Internationa*l, 2013, in press.
[48] Popov V L, Heß M. *Methode der Dimensionsreduktion in der Kontaktmechanik und Reibung.* Berlin: Springer, 2013.
[49] Pohrt R. Private communication.
[50] Heise R, Popov V L. Adhesive contribution to the coefficient of friction between rough surfaces. *Tribology Letters* **39**: 247−250 (2010)
[51] Grosch K A. The relation between the friction and viscoelastic properties of rubber. *Proc R Soc Lond A* **274**: 21−39 (1963)
[52] Ben-David O, Fineberg J. Static friction coefficient is not a material constant. *Phys Rev Lett* **106**: 254301 (2011)
[53] Adams G G, Nosonovsky M. Contact modeling – forces. *Tribology International* **33**: 431−442 (2000)
[54] Psakhie S G, Popov V L. Mesoscopic nature of friction and numerical simulation methods in tribology. *Physical Mesomechanics* **15**: 251−253 (2012)
[55] Filippov A E, Popov V L. Fractal Tomlinson model for mesoscopic friction: From microscopic velocity-dependent damping to macroscopic Coulomb friction. *Physical Review E* **75**: 027103 (2007)
[56] Prandtl L. Ein Gedankenmodell zur kinetischen Theorie der festen Körper. *ZAMM* **8**: 85-106 (1928). English translation: Popov V L, Gray J A T. Prandtl-Tomlinson model: History and applications in friction, plasticity, and nanotechnologies. *ZAMM* **92**: 683–708 (2012)
[57] Popov V L. A theory of the transition from static to kinetic friction in boundary lubrication layers, *Solid State Commun* **115**: 369–373 (2000)
[58] Meyer E, Overney R M, Dransfeld K, Gyalog T. *Nanoscience: Friction and Rheology on the Nanometer Scale.* Singapore: World Scientific, 1998.
[59] Geike T. Theoretische Grundlagen eines schnellen Berechnungsverfahrens für den Kontakt rauer Oberflächen. Ph.D thesis. Berlin: Berlin University of Technology, 2008.
[60] Scaraggi M, Putignano C, Carbone G. Elastic contact of rough surfaces: A simple criterion to make 2D isotropic roughness equivalent to 1D one. *Wear* **297**: 811−817 (2013)

Valentin L. Popov. Full professor at the Berlin University of Technology, studied physics (1976–1982) and obtained his doctorate in 1985 from the Moscow State Lomonosov University. He worked at the Institute of Strength Physics of the Russian Academy of Sciences. After a guest-professorship in the field of theoretical physics at the University of Paderborn (Germany) from 1999 to 2002, he has headed the department of System Dynamics and the Physics of Friction in the Institute of Mechanics at the Berlin University of Technology. His areas of interest include tribology, nanotribology, tribology at low temperatures, biotribology, the influence of friction through ultrasound, numerical simulation of frictional processes, research regarding earthquakes, as well as themes relating to materials sciences such as the mechanics of elastoplastic media with microstructures, strength of metals and alloys, and shape memory alloys. He has published 30 papers in leading international journals during the past 5 years. He is the author of the book "Contact Mechanics and Friction: Physical principles and applications" which appeared in German, English, Chinese, and Russian editions. He is the joint editor of international journals and regularly organizes international conferences and workshops over diverse tribological themes. He is a member of the Scientific Council of the German Tribological Society. He has intensively collaborated with many industrial corporations and possesses experience in implementing the results of scientific research in industrial applications.